Molecular Therapy
Nucleic Acids
Original Article

Identifying Involvement of H19-miR-675-3p-IGF1R and H19-miR-200a-PDCD4 in Treating Pulmonary Hypertension with Melatonin

Ran Wang,[1,7] Sijing Zhou,[2,7] Peipei Wu,[1,7] Min Li,[3] Xing Ding,[1] Li Sun,[1] Xuan Xu,[4] Xuexin Zhou,[5] Luqian Zhou,[5] Chao Cao,[6] and Guanghe Fei[1]

[1]Department of Respiratory and Critical Care Medicine, The First Affiliated Hospital of Anhui Medical University, Hefei 230022, China; [2]Hefei Prevention and Treatment Center for Occupational Diseases, Hefei 230022, China; [3]Department of Oncology, The First Affiliated Hospital of Anhui Medical University, Hefei 230022, China; [4]Division of Pulmonary/Critical Care Medicine, Cedars Sinai Medical Center, Los Angeles, CA 90015, USA; [5]The First Clinical College of Anhui Medical University, Hefei 230032, China; [6]Department of Respiratory Medicine, Ningbo First Hospital, Ningbo 315000, China

Non-coding RNAs play an important role in the pathogenesis of pulmonary arterial hypertension (PAH). The aim of this study was to characterize the therapeutic role of melatonin as well as the underlying molecular mechanism (its effects on the expression of H19 and its downstream signaling pathways) in the treatment of PAH. Real-time PCR and western blot analysis were performed to evaluate the expression of H19, miR-200a, miR-675, insulin-like growth factor-1 receptor (IGF1R), and programmed cell death 4 (PDCD4). The value of systolic pulmonary artery pressure (SPAP) and the ratio of medial thickening in the monocrotaline (MCT) group were increased, whereas the melatonin treatment could decrease these values to some extent. The weights of RV (right ventricle), LV (left ventricle) + IVS (interventricular septal), and RV/(LV + IVS) in the MCT group were much higher than those in the MCT + melatonin and control groups. In addition, the expression of H19, miR-675, IGF1R mRNA, and IGF1R protein in the MCT group was the highest, whereas their expression in the control group was the lowest. The expression of miR-200, PDCD4 mRNA, and PDCD4 protein in the MCT group was the lowest, whereas their expression in the control group was the highest. Furthermore, H19 directly suppressed the expression of miR-200a, whereas miR-675-3p and miR-200a directly inhibited the expression of IGF1R and PDCD4, respectively. Finally, melatonin treatment inhibited cell proliferation; upregulated the expression of H19, miR-675-3p, and PDCD4; and downregulated the expression of miR-200a and IGF1R. This study demonstrated the role of H19-miR-675-3p-IGF1R- and H19-miR-200a-PDCD4-signaling pathways in the melatonin treatment of PAH.

INTRODUCTION

As a multifactorial disease, pulmonary arterial hypertension (PAH) is featured by the continued increase in pulmonary arterial pressure, which finally leads to right ventricular failure and even death.[1] The pathological mechanisms underlying the development of PAH remain complex and unclear. One feature of PAH is the remarkable increase in the resistance of distal small pulmonary arteries (PAs).[2] In pulmonary circulation, the mechanisms underlying the narrowing of low-resistance arterioles include *in situ* thrombosis, pulmonary vascular remodeling, and pulmonary vasoconstriction.[3] Vascular smooth muscle cells (VSMCs) are one of the critical factors affecting vascular homeostasis, and recent studies have shown that the increased proliferation of VSMCs contributes to the structural variations and remodeling of PAH.[4–8] Eddahibi et al.[4,5] demonstrated that multiple genetic and/or environmental factors may cause abnormally enhanced proliferation of VSMCs, forming vascular remodeling, the pathological structure basis of PAH. Vascular remodeling subsequently thickens vessel walls and narrows the lumen of the vessels, leading to an obvious increase in pulmonary arterial resistance.[4–8]

A majority of the known non-coding RNAs (ncRNAs) perform relatively generic functions in cells. For example, small nuclear RNAs (snRNAs) are associated with splicing, small nucleolar RNAs (snoRNAs) are associated with rRNA modification, and both tRNAs and rRNAs are related to the translation of mRNA. Some studies have shown that long ncRNAs (lncRNAs) of 200 nt in length have no or limited protein-coding capacity.[9,10] Nevertheless, it has been demonstrated in some previous investigations that lncRNAs are critical molecules for controlling cellular activities.[11–13] For example, it has been demonstrated that gene expression can be regulated by lncRNAs at the posttranscriptional, epigenetic, and transcriptional levels.[14,15] Furthermore, the expression of H19 lncRNA has been shown to mediate the growth arrest and/or differentiation of SMCs. In

Received 20 April 2018; accepted 18 August 2018;
https://doi.org/10.1016/j.omtn.2018.08.015.

[7]These authors contributed equally to this work.

Correspondence: Guanghe Fei, PhD, Department of Respiratory and Critical Care Medicine, The First Affiliated Hospital of Anhui Medical University, Hefei, 230022, China
E-mail: guanghefei@hotmail.com
Correspondence: Chao Cao, PhD, Department of Respiratory Medicine, Ningbo First Hospital, Ningbo 315000, China
E-mail: caochaoningbo@126.com

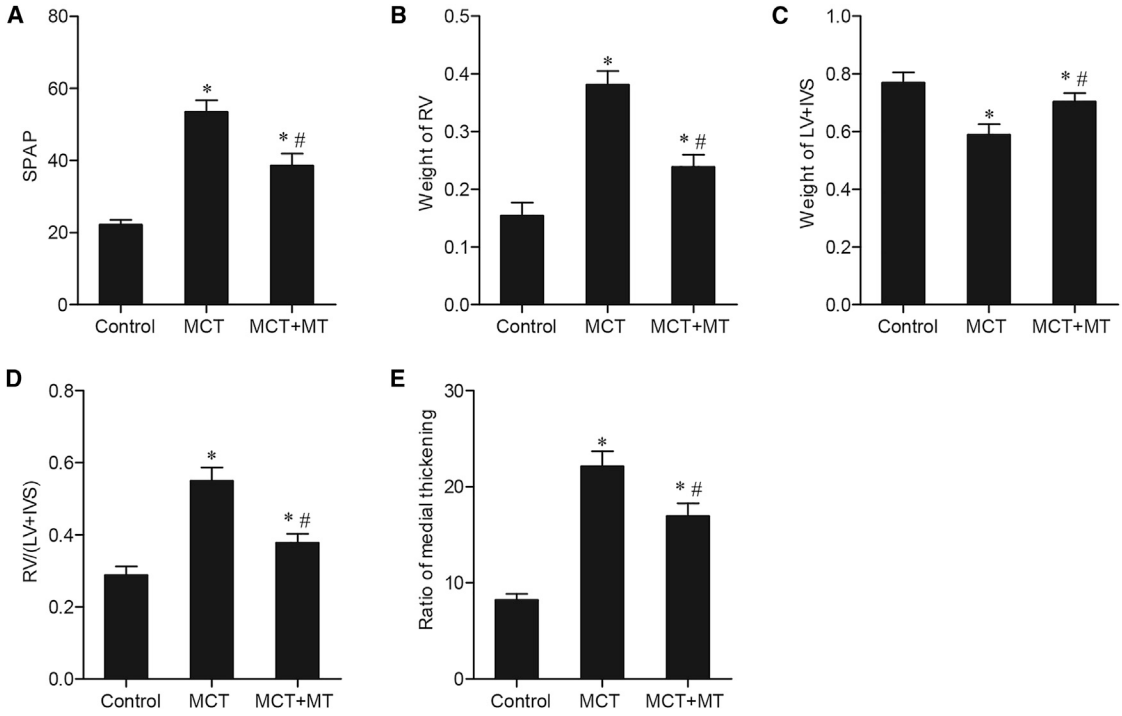

Figure 1. Changes in SPAP and Organ Weights after MCT Treatment in PAH Rats

(A) SPAP in the MCT group was much higher than in the MCT plus melatonin group, and both of them were much higher than the control group (*p < 0.05 as compared with the control group, #p < 0.05 as compared with the MCT group). (B) Weight of RV in the MCT group was much higher than in the MCT plus melatonin and control groups, and both of them were higher than that of the control group (*p < 0.05 as compared with the control group, #p < 0.05 as compared with the MCT group). (C) The MCT group exhibited a lower weight of LV + IVS compared with the MCT plus melatonin group, and the MCT plus melatonin group showed a lower weight of LV + IVS than the control group (*p < 0.05 as compared with the control group, #p < 0.05 as compared with the MCT group). (D) The MCT group exhibited a higher RV/(LV + IVS) compared with the MCT plus melatonin group, and the MCT plus melatonin group showed a higher RV/(LV + IVS) than the control group (*p < 0.05 as compared with the control group, #p < 0.05 as compared with the MCT group). (E) Ratio of medial thickening in the MCT group was much higher than in the MCT plus melatonin group, and both of them were much higher than the control group (*p < 0.05 as compared with the control group, #p < 0.05 as compared with the MCT group).

addition, it was discovered by Wiles[16] that some genes in undifferentiated embryonal carcinoma cells remain silent and only start to express themselves when the cells have differentiated into the endoderm. Also, in the multipotential mesodermal embryonic cell line C3H lOT 1/2 that can be used to simulate different stages of muscle cell development, the expression of H19 gene dramatically increases when precursor stem cells differentiate into myoblasts.[17]

As a hormone also named N-acetyl-5-methoxy tryptamine,[1] melatonin is secreted by the pineal gland in animals and regulates the natural sleep cycle.[18] Melatonin primarily exerts its biological effect through melatonin receptors, although it can also act as an antioxidant to protect mitochondrial and nuclear DNA.[19]

Previous investigations have demonstrated that chronic hypoxia leads to a significantly elevated level of lipid peroxidation in the lungs.[20,21] In addition, during chronic hypoxia, progenitor cells migrate into pulmonary vascular walls and, hence, result in medial thickening.[22] As a hormone well known for its high lipophilicity and ability to scavenge free radicals, melatonin can reduce the oxidative stress level and relieve pulmonary hypertension.[23]

It has been shown that melatonin treatment could upregulate the expression of H19 and miR-675, whereas H19 could bind to miR-200a competitively to inhibit the expression of miR-200a.[24,25] In addition, by searching online microRNA (miRNA) databases (http://www.mirdb.org and http://mirtarbase.mbc.nctu.edu.tw/php/index.php), we have identified insulin-like growth factor-1 receptor (IGF1R) and programmed cell death 4 (PDCD4) as possible target genes for miR-675-3p and miR-200a, respectively. In this study, we established animal models of PAH and investigated the therapeutic effect of melatonin in the treatment of PAH as well as its effect on the expression of H19 and its downstream signaling pathways.

RESULTS

Changes in SPAP and Organ Weights after MCT Treatment

The rats were treated with monocrotaline (MCT) to establish a rat model of PAH. Subsequently, the PAH rats were treated with melatonin, and the values of systolic pulmonary artery pressure (SPAP), right ventricle (RV), left ventricle (LV) + interventricular septal (IVS), and RV/(LV + IVS), as well as the ratio of medial thickening in the control, MCT, and MCT + melatonin groups, were measured. As shown in Figure 1, the SPAP value and ratio of medial thickening

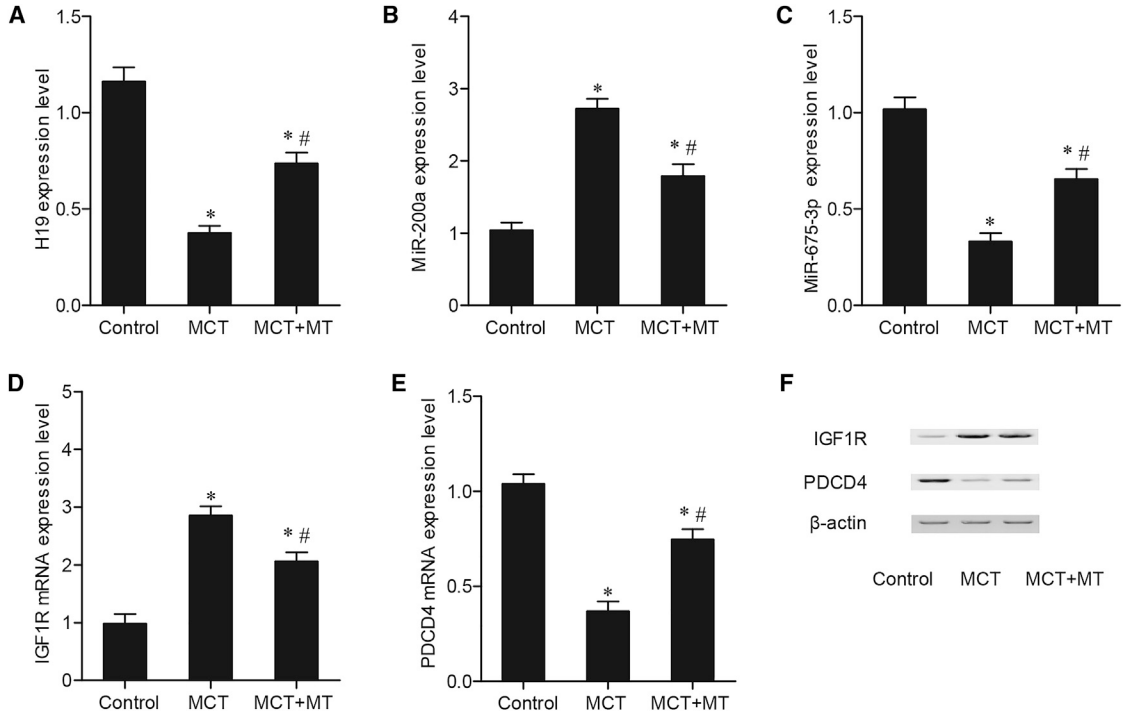

Figure 2. Differential Levels of H19, miR-675, miR-200a, IGF1R, and PDCD4 after MCT Treatment in PAH Rats

(A) The H19 level in the MCT plus melatonin group was much higher than in the MCT group, while it was even higher in the control group than in the MCT plus melatonin group (*$p < 0.05$ as compared with the control group, #$p < 0.05$ as compared with the MCT group). (B) The miR-200a level in the MCT plus melatonin group was much higher than in the control group, while it was even higher in the MCT group than in the MCT plus melatonin group (*$p < 0.05$ as compared with the control group, #$p < 0.05$ as compared with the MCT group). (C) The miR-675-3p level in the MCT group was much lower than in the MCT plus melatonin group, and both of them were much lower than in the control group (*$p < 0.05$ as compared with the control group, #$p < 0.05$ as compared with the MCT group). (D) The IGF1R mRNA level in the MCT group was much higher than in the MCT plus melatonin group, and both of them were much higher than in the control group (*$p < 0.05$ as compared with the control group, #$p < 0.05$ as compared with the MCT group). (E) The MCT plus melatonin group displayed a lower level of PDCD4 mRNA than did the control group, while the MCT group exhibited an even lower level of PDCD4 mRNA than did the MCT plus melatonin group (*$p < 0.05$ as compared with the control group, #$p < 0.05$ as compared with the MCT group). (F) The IGF1R protein level in the MCT group was much higher than in the MCT plus melatonin group, and both of them were much higher than in the control group. The PDCD4 protein level in the MCT group was much lower than in the MCT plus melatonin group, and both of them were much lower than in the control group (*$p < 0.05$ as compared with the control group, #$p < 0.05$ as compared with the MCT group).

in the control group were the lowest, whereas the SPAP value (Figure 1A) and ratio of medial thickening (Figure 1E) in the MCT group were the highest. Meanwhile, weights of RV (Figure 1B), LV + IVS (Figure 1C), and RV/(LV + IVS) (Figure 1D) in MCT-treated rats were evidently increased, whereas the treatment with melatonin decreased the corresponding values.

Different Levels of H19, miR-675-3p, miR-200a, IGF1R, and PDCD4 after MCT Treatment

The expression of H19, miR-675-3p, miR-200a, IGF1R, and PDCD4 among the control, MCT, and MCT + melatonin groups was determined by real-time PCR and western blot analysis. As shown in Figure 2, the expression of miR-200a (Figure 2B), IGF1R mRNA (Figure 2D), and IGF1R protein (Figure 2F) in the MCT group was the highest, whereas their expression in the control group was the lowest. In contrast, the expression of H19 (Figure 2A), miR-675-3p (Figure 2C), PDCD4 mRNA (Figure 2E), and PDCD4 protein (Figure 2F) in the MCT group was the lowest, whereas their expression in the control group was the highest.

Protein Expression of IGF1R and PDCD4 in the Control, MCT, and MCT + Melatonin Groups

Immunohistochemistry (IHC) assays were carried out to measure the protein level of IGF1R and PDCD4 in the control, MCT, and MCT + melatonin groups. As shown in Figure 3, IGF1R protein expression in the MCT group was the highest, whereas its expression in the control group was the lowest. In contrast, as shown in Figure 4, PDCD4 protein expression in the MCT group was the lowest, whereas its expression in the control group was the highest.

H19 Directly Regulates the Expression of miR-200a

A computational analysis was performed to investigate whether H19 served as molecular sponges or as competing endogenous RNAs in the regulation of miR-200a expression. As shown in Figure 5A, a putative binding site of H19 was located on miR-220a. Subsequently,

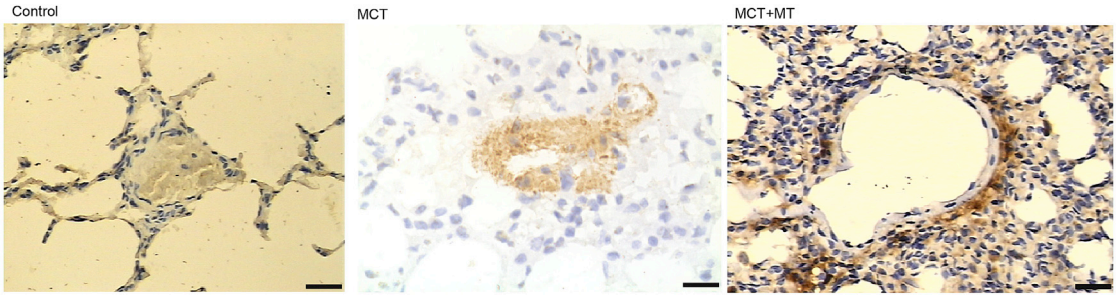

Figure 3. Immunohistochemistry for IGF1R

According to the IHC result, the IGF1R protein level in the MCT group was much higher than in the MCT plus melatonin group, and both of them were much higher than in the control group (scale bars, 10 μm).

luciferase assays were conducted to further confirm the regulatory relationship between H19 and miR-200a in human pulmonary artery smooth muscle cells (hPASMCs) and rat PASMCs (rPASMCs). Compared with scramble control, miR-200a mimics significantly reduced luciferase activity of wild-type H19 in hPASMCs (Figure 5B) and rPASMCs (Figure 5C), whereas the luciferase activity of mutant H19 in hPASMCs (Figure 5B) and rPASMCs (Figure 5C) transfected with miR-200a mimics showed no significant difference, suggesting that H19 negatively regulated miR-200a expression.

miR-675-3p and miR-200a Directly Targeted IGF1R and PDCD4, Respectively

We performed a computational analysis to investigate the role of miR-675-3p and miR-200a in PAH. IGF1R (Figure 6A) and PDCD4 (Figure 6D) were identified as target genes of miR-675-3p and miR-200a, respectively. As compared with the cells transfected with the scramble control, miR-675-3p mimics significantly inhibited the luciferase activity of wild-type IGF1R 3′ UTR in hPASMCs (Figure 6B) and rPASMCs (Figure 6C), whereas the luciferase activity of mutant IGF1R 3′ UTR in hPASMCs and rPASMCs transfected with miR-675-3p mimics showed no significant difference. In addition, miR-200a mimics significantly inhibited the luciferase activity of wild-type PDCD4 3′ UTR in hPASMCs (Figure 6E) and rPASMCs (Figure 6F), whereas the luciferase activity of mutant PDCD4 3′ UTR in hPASMCs and rPASMCs transfected with miR-200a mimics showed no significant difference. Collectively, these results indicated that miR-675-3p and miR-200a directly targeted IGF1R and PDCD4, respectively.

Effect of Melatonin on Cell Proliferation and Expression of H19, miR-675-3p, miR-200a, IGFIR, and PDCD4

Different doses of melatonin (1 nM, 100 nM, and 10 μM) were used to treat hPASMCs and rPASMCs. Subsequently, MTT (3-(4,5-dimethyl-2-thiazolyl)-2,5-diphenyl-2-H-tetrazolium bromide) assay, real-time PCR, and western blot analyses were utilized to detect cell proliferation and the expression of H19, miR-675-3p, miR-200a, IGFIR, and PDCD4. As shown in Figures 7 and 8, melatonin treatment decreased the growth rate of hPASMCs (Figures 7A and 7B) and rPASMCs (Figures 8A and 8B) in a dose-dependent manner. In addition, the expression of H19 (Figures 7C and 8C), miR-675-3p (Figures 7D and 8D), PDCD4 mRNA (Figures 7G and 8G), and PDCD4 protein (Figures 7H and 8H) in hPASMCs (Figure 7) and rPASMCs (Figure 8) was increased with melatonin treatment in a dose-dependent manner. Contradictorily, miR-200a expression (Figures 7E and 8E), IGF1R mRNA (Figures 7F and 8F), and IGF1R protein (Figures 7H and 8H) in hPASMCs (Figure 7) and rPASMCs (Figure 8) was reduced with melatonin treatment in a dose-dependent manner. Overall, these findings indicated the involvement of two signaling pathways (H19-miR-675-IGFR1 and H19-miR-200a-PDCD4) in the therapeutic role of melatonin, which alleviated the severity of PAH by promoting the apoptosis of PASMCs (Figure 9).

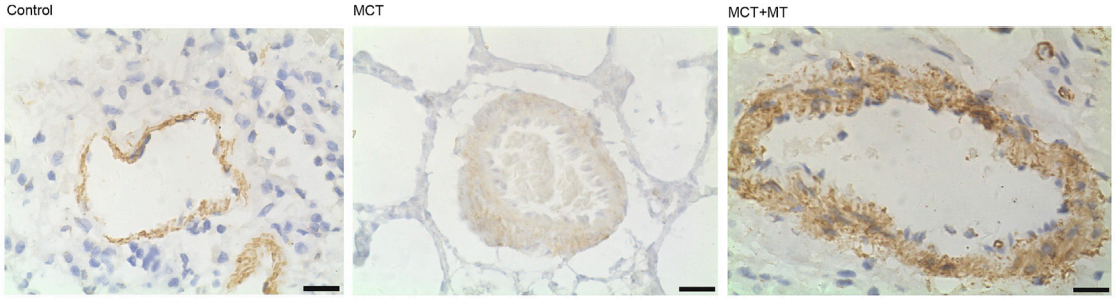

Figure 4. Immunohistochemistry for PDCD4

According to the IHC result, the PDCD4 protein level in the MCT group was much lower than in the MCT plus melatonin group, and both of them were much lower than in the control group (scale bars, 10 μm).

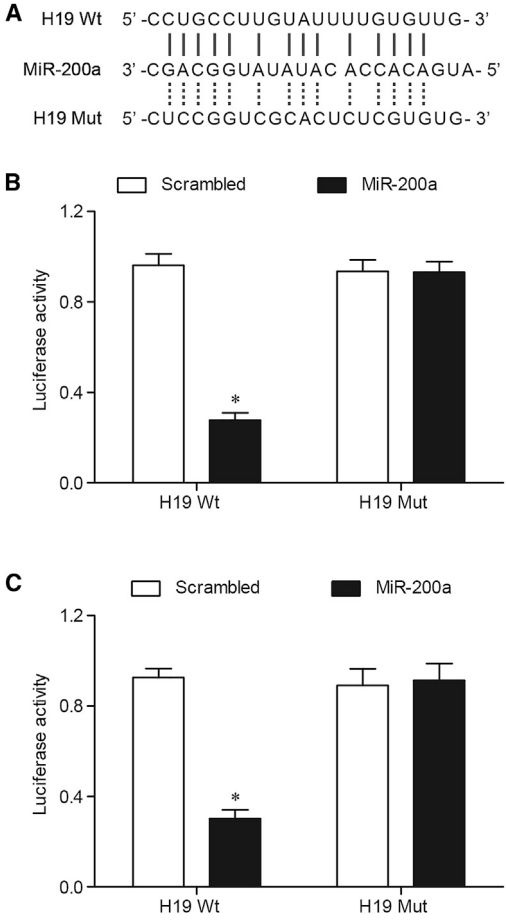

Figure 5. H19 Directly Regulated miR-200a

(A) Comparison of the sequences of H19 and mutant with replacement of binding site against the sequence of miR-200a. (B) miR-200a mimic inhibited luciferase activity of wild-type H19, but not that of mutant H19 in hPASMCs (*$p < 0.05$ as compared with the control group). (C) miR-200a mimic reduced luciferase activity of wild-type H19 compared with scramble control, and luciferase activity of mutant H19 showed no obvious difference with scramble control in rPASMCs (*$p < 0.05$ as compared with the control group).

DISCUSSION

Melatonin, chemically known as *N*-acetyl-5-methoxy tryptamine, is a hormone produced by the pineal gland in animals and regulates the natural sleep cycle.[22,23,26] It has been shown that the administration of melatonin could treat PAH by suppressing the proliferation of PASMCs or by ameliorating the level of oxidation, although the molecular mechanism underlying melatonin treatment remains elusive.[21,27] In this study, a rat model of PAH was established by injecting the rats with MCT. The successful establishment of the animal model was verified by measuring the value of SPAP and the weights of RV, LV + IVS, and RV/(LV + IVS).

It has been shown that, due to the presence of melatonin, hydrogen peroxide (H_2O_2) cannot suppress the expression of H19 mRNA in cardiac progenitor cells (CPCs). In addition, H19 was shown to be involved in melatonin's protection against aging in CPCs. Nevertheless, this study is the first to show that melatonin regulates the expression of lncRNAs. As a primary precursor of miRNA-675, H19 produces two mature forms, miR-675-3p (referred to as miR-675*) and miR-675-5p (referred to as miR-675), in a classic manner dependent on Drosha and Dicer splicing.[28] miR-675-3p was found to promote the proliferation of colon cancer cells,[29] whereas H19 acts as a growth inhibitor in embryonic development.[30]

In this study, it was found that the expression of H19, miR-675-3p, and IGF1R in the MCT group was the highest, whereas their expression was the lowest in the control group. In addition, the expression of miR-200 and PDCD4 in the MCT group was the lowest, whereas their expression was the highest in the control group. Furthermore, the luciferase reporter assays showed that the overexpression of miR-200a repressed the luciferase activity in cells transfected with full-length H19, whereas the site-directed mutagenesis of the miR-200a-binding site successfully abrogated the inhibitory effect of miR-200a. Overall, these results suggested that H19 acts as a target of miR-200a.

As a member of the insulin or IGF family, IGF-1, a single-chain polypeptide with a high sequence homology to pro-insulin, plays a pivotal role in the regulation of metabolism, differentiation, postnatal development, and overall growth of an organism. IGF-1 is expressed in most cells, and it regulates the migration, survival, differentiation, growth, proliferation, apoptosis, and adhesion of the cells. For example, IGF-1 promotes the growth of SMCs and suppresses their apoptosis *in vitro*.[31] In pulmonary artery, IGF-1 inhibits the apoptosis of SMCs by increasing the expression of MAPK, iNOS, and p38.[31] In addition, IGF-1 can activate elastin in VSMCs, and the increased expression of IGF-1 has been linked to the remodeling of neonatal pulmonary hypertension (PH) in sheep models.[32–34]

PDCD4 is a key mediator of apoptosis. Stimuli or genetic mutations, which downregulate the expression of PDCD4, are linked to the progression of cancer and the proliferation of VSMCs following carotid injury.[35–38] PDCD4 also regulates the apoptosis of endothelial cell (EC), vascular remodeling, and the development of intimal hyperplasia.[39,40] In this study, it is hypothesized that, as a main mediator of apoptosis, the expression and activity of PDCD4 is improved by H_2O_2, thus enhancing the susceptibility of hPASMCs to apoptosis and repressing their proliferation upon hypoxia. In addition, as a key mediator of proliferation in hPASMCs exposed to hypoxia, miR-200a also downregulates the expression of PDCD4 by binding to the 3′ UTR of PDCD4.[41–43] In fact, miR-21 has been shown to suppress the translation of PDCD4 during systemic vascular injury, cancer cell proliferation, hPASMC proliferation, and endothelial apoptosis.[37,44–47]

Apoptosis has been demonstrated to considerably reverse hypoxic pulmonary arterial remodeling during re-oxygenation, although the key cells involved in such processes have not been fully defined.[48] It is well known that the reduced apoptosis and enhanced proliferation of PASMCs in small pulmonary arteries could result in pulmonary

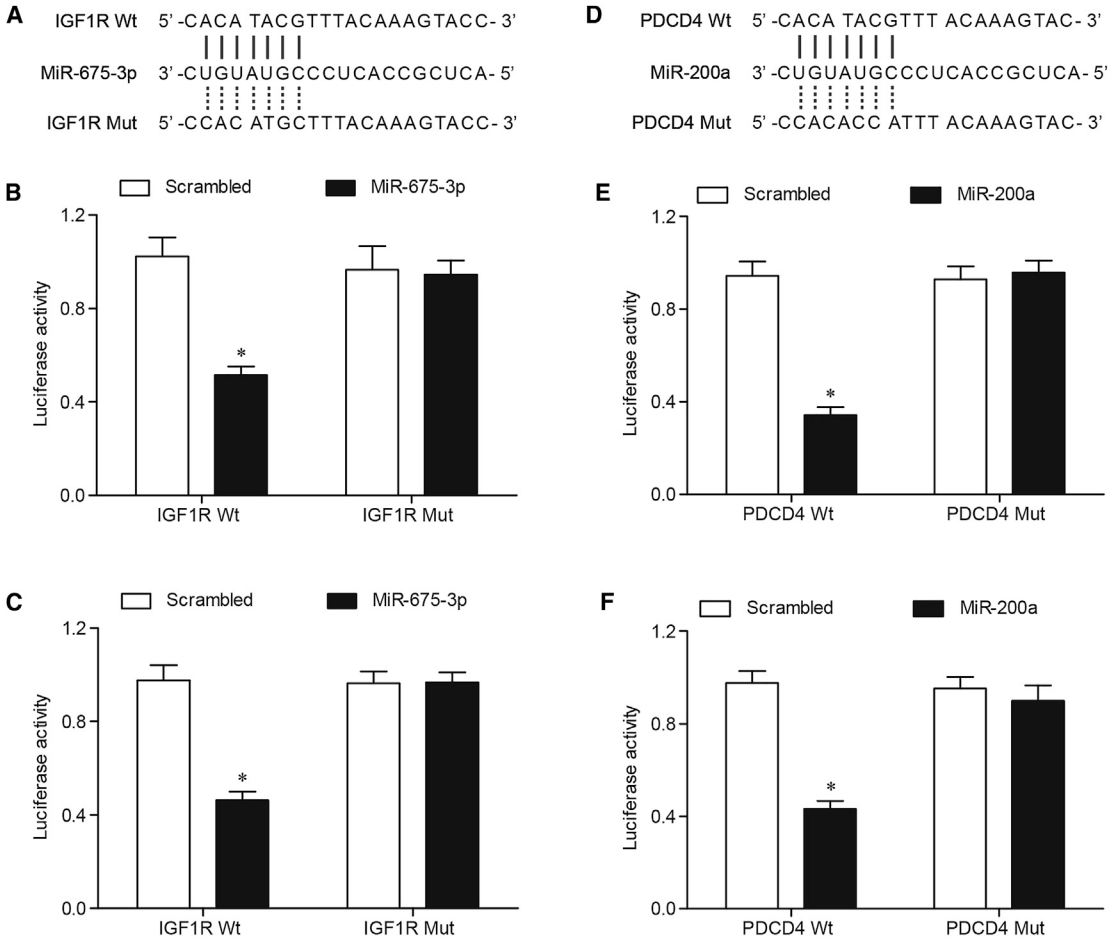

Figure 6. miR-675-3p and miR-200a Directly Targeted IGF1R and PDCD4, Respectively

(A) The sequence comparison between mature miR-675-3p and wild-type as well as mutant IGF1R 3′ UTR. (B) Luciferase activity of wild-type IGF1R 3′ UTR, but not that of mutant IGF1R 3′ UTR, in hPASMCs transfected with miR-675-3p mimic was much lower than scramble control (*$p < 0.05$ as compared with the control group). (C) Luciferase activity of wild-type IGF1R 3′ UTR, but not that of mutant IGF1R 3′ UTR, in rPASMCs transfected with miR-675 mimic was much lower than scramble control (*$p < 0.05$ as compared with the control group). (D) The sequence comparison between mature miR-200a and wild-type as well as mutant PDCD4 3′ UTR. (E) Luciferase activity of wild-type PDCD4 3′ UTR, but not that of mutant PDCD4 3′ UTR, in hPASMCs transfected with miR-675 mimic was downregulated compared with scramble control (*$p < 0.05$ as compared with the control group). (F) Transfecting with miR-200a mimic reduced luciferase activity of wild-type PDCD4 3′ UTR, but not that of mutant PDCD4 3′ UTR, in rPASMCs (*$p < 0.05$ as compared with the control group).

arterial remodeling upon hypoxia, although the thickened medial layer could restore to its normal dimension during re-oxygenation.[49–51] In addition, it has been demonstrated in previous studies that induced apoptosis of PASMCs could reverse pulmonary vascular remodeling.[52–54] Nevertheless, it remains unknown whether the increased apoptosis of PASMCs is involved in the reversal of pulmonary arterial remodeling during re-oxygenation.

There are limitations to this study. First, the functional analysis was mainly performed in an animal model of PAH by administrating MCT, which only represents one type of PAH model, and the therapeutic effect of melatonin and its effect on H19 and downstream signaling pathways should also be confirmed in other animal model of PAHs, such as hypoxic PAH. Second, the therapeutic effect of melatonin should also be verified in human subjects, which is one of necessary steps before the medicine could be used clinically to treat PAH.

This present study is a pilot study to explore the possibility for melatonin to be used to treat PAH, and both lncRNA (H19) and miRNAs (miR-675 and miR-200a) could be therapeutic targets in the management of PAH.

In summary, the findings of this present study demonstrated that H19 mediated the therapeutic effect of melatonin in the treatment of PAH via regulating two signaling pathways (H19-miR-675-3p-IGF1R and H19-miR-200a-PDCD4), and we showed that the administration of melatonin upregulated the expression of H19 and miR-675-3p and downregulated the expression of miR-200a, resulting in an increased

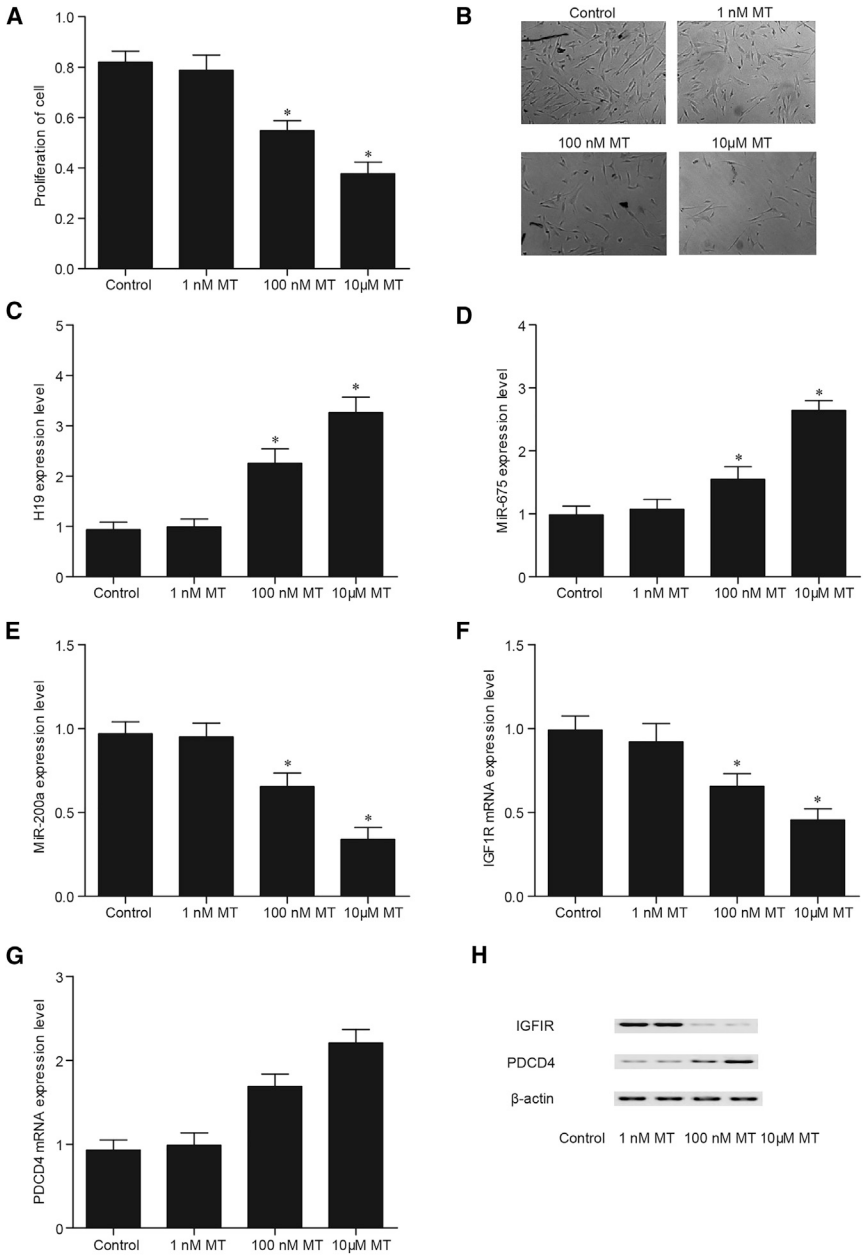

Figure 7. Effect of Melatonin on Cell Proliferation and H19, miR-675-3p, miR-200a, IGF1R, and PDCD4 Levels in hPASMCs

(A) Melatonin inhibited cell viability of hPASMCs in a dose-dependent manner (*$p < 0.05$ as compared with the control group). (B) Melatonin inhibited cell viability of hPASMCs in a dose-dependent fashion. (C) Treating with melatonin dose-dependently upregulated H19 expression (*$p < 0.05$ as compared with the control group). (D) Treating with melatonin dose-dependently enhanced miR-675-3p expression (*$p < 0.05$ as compared with the control group). (E) miR-200a level was dose-dependently reduced following treatment with melatonin (*$p < 0.05$ as compared with the control group). (F) IGF1R mRNA level was dose-dependently suppressed after the administration of melatonin (*$p < 0.05$ as compared with the control group). (G) PDCD4 mRNA level was dose-dependently upregulated subsequent to treatment with melatonin (*$p < 0.05$ as compared with the control group). (H) IGF1R protein level was dose-dependently suppressed while PDCD4 protein expression was dose-dependently enhanced following treatment with melatonin.

expression of PDCD4 and a decreased expression of IGFR1. Such changes in the expression of PDCD4 and IGF1R lead to the promoted apoptosis and the suppressed proliferation of PASMCs, to alleviate vascular remodeling and PAH.

MATERIALS AND METHODS

Establishment of a PAH Animal Model via MCT Administration

Animal experiments were carried out following protocols approved by the Institutional Animal Care and Use Committee of Anhui Medical University. The experiments were performed as previously described.[55] 40 healthy male rats, which were 10 weeks old and 200–250 g in weight, were obtained from Anhui Medical University. 60 mg kg^{-1} MCT was injected into the rats to establish a PAH model. Melatonin (Sigma-Aldrich, St. Louis, MO, USA) was dissolved in indoleamine-containing absolute ethanol and further diluted with normal saline (2% ethanol in normal saline). Subsequently, melatonin was intraperitoneally injected into PAH rats at a frequency of 1 injection/day with a dose of 10 mg/kg body weight.

RNA Isolation and Real-Time PCR

The experiments were performed as previously described.[56,57] TRIzol reagent (Invitrogen, Carlsbad, CA, USA) was used to extract total RNA from PASMCs or tissue samples. An All-in-One miRNA qRT-PCR Detection Kit (GeneCopoeia, Rockville, MD, USA) was used to determine the relative expression of H19, miR-200a, and miR-675-3p that has been normalized to the expression of small RNA U6. In addition, a PrimerScript RT reagent kit (Takara, Dalian, China) was used to synthesize cDNA from extracted RNA, followed by SYBR green qRT-PCR reactions (LightCycler480, Roche, Basel, Switzerland) to determine the mRNA expression of IGF1R and PDCD4 that has been normalized to the expression of GAPDH. The $2^{-\Delta\Delta CT}$ method was used to calculate the relative expression of H19, miR-200a, miR-675-3p, IGFIR, and PDCD4 mRNA. The primer sets used for real-time PCR were as follows: H19 forward 5′-GCCG AGTTCGCTAGGCAAGCA-3′ and reverse 5′-CTCAACTGGTGTC GTGGA-3; miR-200a forward 5′-GCCGAGTGGTGCGGAGAGG GC-3′ and reverse 5′-CTCAACTGGTGTCGTGGA-3′; miR-675-3p

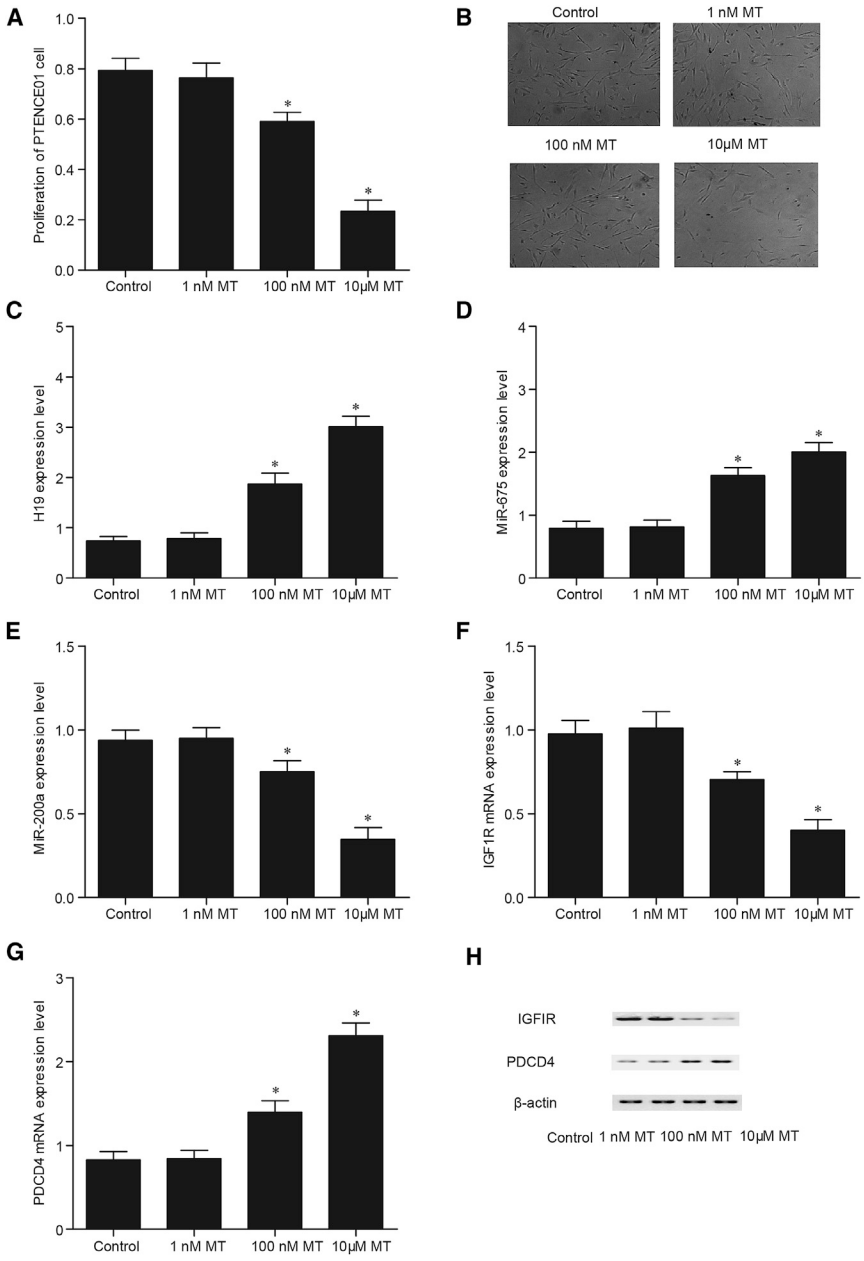

Figure 8. Effect of Melatonin on Cell Proliferation and H19, miR-675, miR-200a, IGF1R, and PDCD4 Levels in rPASMCs

(A) Melatonin inhibited cell viability of rPASMCs in a dose-dependent manner (*$p < 0.05$ as compared with the control group). (B) Melatonin inhibited cell viability of rPASMCs in a dose-dependent fashion. (C) Treating with melatonin dose-dependently upregulated H19 expression (*$p < 0.05$ as compared with the control group). (D) Treating with melatonin dose-dependently enhanced miR-675-3p expression (*$p < 0.05$ as compared with the control group). (E) miR-200a level was dose-dependently reduced following treatment with melatonin (*$p < 0.05$ as compared with the control group). (F) IGF1R mRNA level was dose-dependently suppressed after the administration of melatonin (*$p < 0.05$ as compared with the control group). (G) PDCD4 mRNA level was dose-dependently upregulated subsequent to treatment with melatonin (*$p < 0.05$ as compared with the control group). (H) IGF1R protein level was dose-dependently suppressed while PDCD4 protein expression was dose-dependently enhanced following treatment with melatonin.

forward 5′-GCCGAGCATCTTACCGGACGT-3′ and reverse 5′-CTCAACTGGTGTCGTGGA-3′; PDCD4 forward 5′-GCAAAAAGGCGACTAAGGAAAAA-3′ and reverse 5′-TAAGGGCGTCACTCCCACT-3′; and IGF1R forward 5′-TCGACATCCGCAACGACTATC-3′ and reverse 5′-TCGACATCCGCAACGACTATC-3′. All reactions were carried out in triplicates.

Cell Culture and Transfection

The experiments were performed as previously described.[58,59] hPASMCs and rPASMCs were cultured in an RPMI-1640 medium containing 10% fetal bovine serum (FBS), glutamine, streptomycin (100 mg/mL), and penicillin G (100 U/mL). The cells were incubated at 37°C in a humidified incubator containing 5% CO_2/95% air. The PASMCs were treated with melatonin. When the cells were 70%–80% confluent, hPASMCs and rPASMCs were transfected with 100 nM mimics of H19, miR-200a, and miR-675-3p. All experiments were repeated three times.

Cell Proliferation Assay

The experiments were performed as previously described.[60,61] Briefly, PASMCs were seeded into 24-well plates and treated accordingly before an MTT cell proliferation assay kit (Sigma-Aldrich, St. Louis, MO, USA) was used to assay cell viability. Each experiment was performed in triplicates.

Luciferase Assay

The experiments were performed as previously described.[62] Luciferase assay was performed to determine the interaction among H19, miRNAs, and the target genes. In brief, the full-length H19 was synthesized on an Expand High Fidelity PCR system (Roche Molecular Diagnostics, Basel, Switzerland) and inserted into a pMIR-REPORT vector (Applied Biosystems, Waltham, MA, USA) immediately upstream of the luciferase reporter gene. This vector was termed wild-type H19 vector. Subsequently, a QuikChange Lightening Site-Directed Mutagenesis Kit (Stratagene, La Jolla, CA, USA) was utilized to mutate the H19, and a mutant-type H19 vector was generated by inserting the mutated H19 into the same location of the pMIR-REPORT vector. hPASMCs and rPASMCs were seeded into 48-well plates at a density of 5×10^4

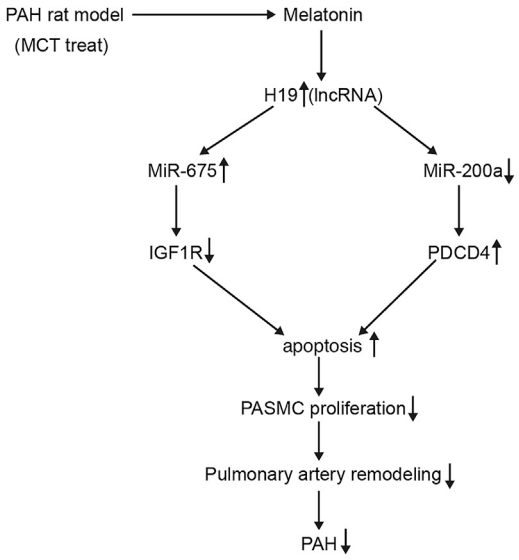

Figure 9. Two Signaling Pathways Are Shown

Dual signaling pathways (H19-miR-675-3p-IGF1R and H19-miR-200a-PDCD4) were involved in the mechanisms underlying the therapeutic effect of melatonin in the treatment of PAH by promoting the apoptosis of PASMCs.

cells/well before they were co-transfected with 5 ng luciferase reporter construct (firefly luciferase) and miR-200a mimics, using Lipofectamine 2000 (Invitrogen, Carlsbad, CA, USA). At 48 hr after the transfection, 200 μL passive lysis buffer (Promega, Madison, WI, USA) was used to harvest the cells. A Dual-Glo luciferase assay system (Promega, Madison, WI, USA) was utilized to detect the activities of firefly and renilla luciferase in the cells. Each experiment was repeated three times.

Similarly, the UTR fragments of PDCD4 and IGFIR were obtained -using PCR amplification on the Expand High Fidelity PCR system. Subsequently, PCR products were purified with agarose gel electrophoresis and inserted into the pMIR-REPORT vector immediately downstream of the luciferase reporter gene. The binding sites for miR-200a and miR-675-3p on the PDCD4 and IGFIR 3′ UTR were mutated, respectively. hPASMCs and rPASMCs were seeded into 48-well plates at a density of 5×10^4 cells/well, and they were transfected with 5 ng luciferase reporter construct (firefly luciferase) plus miR-200a or miR-675-3p mimics using Lipofectamine 2000. At 48 hr after the transfection, 200 μL passive lysis buffer (Promega, Madison, WI, USA) was used to harvest the cells. A Dual-Glo luciferase assay system (Promega, Madison, WI, USA) was utilized to detect the activities of firefly and renilla luciferase in the cells. Each experiment was repeated three times.

Western Blot Analysis

The experiments were performed as previously described.[63] At 48 hr after transfection, hPASMCs and rPASMCs were lysed in a radioimmunoprecipitation assay (RIPA) buffer containing a protease inhibitor cocktail (Sigma-Aldrich, St. Louis, MO, USA). Subsequently, the lysate was centrifuged for 15 min at 14,000 rpm. The total protein in the lysate was separated using 10% SDS-PAGE and electro-transferred onto a polyvinylidene fluoride (PVDF) membrane (Millipore, Billerica, MA, USA). In the next step, the membrane was washed three times in Tris-buffered saline (TBS) containing 0.5% Tween-20, and blocked at room temperature for 2 hr in TBST containing 5% non-fat milk. Subsequently, the membrane was incubated at 4°C for 12 hr with anti-β-actin monoclonal antibodies (1:8,000 dilution, Santa Cruz Biotechnology, Santa Cruz, CA, USA) or polyclonal goat primary antibodies against PDCD4 and IGF1R (1:5,000 dilution, Santa Cruz Biotechnology, Santa Cruz, CA, USA). After incubation, the membrane was washed three times in TBST before incubating with HRP (horseradish peroxidase)-linked anti-goat secondary antibodies (1:10,000 dilution, Santa Cruz Biotechnology, Santa Cruz, CA, USA) at room temperature for 2 hr. An ECL PlusWestern Blotting Detection System (Amersham, Buckinghamsire, UK) was utilized to expose the film and visualize the chemiluminescence. ImageJ software (NIH, Bethesda, MD, USA) was utilized to analyze the protein bands. Three independently experiments were carried out.

Analysis of Apoptosis

PASMCs were transfected with miR-675-3p or miR-200a mimics and seeded into 6-well plates at a density of 2×10^3 cells per well. An Annexin-V-Fluos and Propidium Iodide (PI) Apoptosis Detection Kit (Sigma-Aldrich, St. Louis, MO, USA) was used to evaluate the apoptosis of cells on a fluorescence-activated cell sorter (BD Biosciences, San Jose, CA, USA). All experiments were repeated at least three times.

IHC Assay

The experiments were performed as previously described.[64,65] The tissue samples were fixed in 4% paraformaldehyde, dehydrated, embedded in paraffin, and sliced into 4-μm sections. Subsequently, the sections were blocked with 3% H_2O_2 to inactivate the activity of endogenous peroxidase, followed by incubation at room temperature for 2 hr with primary goat antibodies against PDCD4 (1:200 dilution, Santa Cruz Biotechnology, Santa Cruz, CA, USA) and IGF1R (1:200 dilution, Santa Cruz Biotechnology, Santa Cruz, CA, USA). After the incubation, the sections were washed three times in TBST and incubated at room temperature for 1 hr with HRP-linked anti-goat secondary antibodies (1:1,000 dilution, Santa Cruz Biotechnology, Santa Cruz, CA, USA). Finally, the sections were stained with a DAB (3, 3-diaminobenzidine) substrate kit (Vector Laboratories, Burlingame, CA, USA) and counterstained with hematoxylin. All tests were repeated three times.

Statistical Analysis

All data are presented as mean ± SD. The differences among different groups were evaluated by using one-way ANOVA (when compared among three or more groups), Student Newman Keuls method (when compared between two groups), and Mann-Whitney test (a non-parametric method). All statistical analyses were conducted using SPSS version 14.0 for windows (SPSS, Chicago, IL, USA). A p value of < 0.05 was considered statistically significant.

AUTHOR CONTRIBUTIONS

R.W. designed and carried out most of the experiments, analyzed the data, and wrote the manuscript. S.Z. and P.W. acquired, analyzed, and interpreted data and drafted the manuscript. M.L., X.D., L.S., X.X., X.Z., and L.Z. were responsible for the concept, analyzed and interpreted data, and performed critical revision of the manuscript. G.F. and C.C. helped to design and coordinate the experiment.

CONFLICTS OF INTEREST

The authors have no conflict of interest.

ACKNOWLEDGMENTS

This research was supported by the fund from the Natural Science Foundation of China (81300041), the fund for the academic backbone of the excellent young and middle-age people of Anhui Medical University (2013), the fund from The First Affiliated Hospital of Anhui Medical University for reserve talents (2014), and the fund for Excellent Top Talent Cultivation Project of Anhui Higher Education Institutions (gxyqZD2017030).

REFERENCES

1. Schön, P. (2018). Atomic force microscopy of RNA: State of the art and recent advancements. Semin. Cell Dev. Biol. *73*, 209–219.
2. Jacob, F., and Monod, J. (1961). Genetic regulatory mechanisms in the synthesis of proteins. J. Mol. Biol. *3*, 318–356.
3. Rivas, E., Klein, R.J., Jones, T.A., and Eddy, S.R. (2001). Computational identification of noncoding RNAs in E. coli by comparative genomics. Curr. Biol. *11*, 1369–1373.
4. Eddahibi, S., Guignabert, C., Barlier-Mur, A.M., Dewachter, L., Fadel, E., Dartevelle, P., Humbert, M., Simonneau, G., Hanoun, N., Saurini, F., et al. (2006). Cross talk between endothelial and smooth muscle cells in pulmonary hypertension: critical role for serotonin-induced smooth muscle hyperplasia. Circulation *113*, 1857–1864.
5. Dewachter, L., Adnot, S., Fadel, E., Humbert, M., Maitre, B., Barlier-Mur, A.M., Simonneau, G., Hamon, M., Naeije, R., and Eddahibi, S. (2006). Angiopoietin/Tie2 pathway influences smooth muscle hyperplasia in idiopathic pulmonary hypertension. Am. J. Respir. Crit. Care Med. *174*, 1025–1033.
6. Guignabert, C., Alvira, C.M., Alastalo, T.P., Sawada, H., Hansmann, G., Zhao, M., Wang, L., El-Bizri, N., and Rabinovitch, M. (2009). Tie2-mediated loss of peroxisome proliferator-activated receptor-gamma in mice causes PDGF receptor-beta-dependent pulmonary arterial muscularization. Am. J. Physiol. Lung Cell. Mol. Physiol. *297*, L1082–L1090.
7. Izikki, M., Guignabert, C., Fadel, E., Humbert, M., Tu, L., Zadigue, P., Dartevelle, P., Simonneau, G., Adnot, S., Maitre, B., et al. (2009). Endothelial-derived FGF2 contributes to the progression of pulmonary hypertension in humans and rodents. J. Clin. Invest. *119*, 512–523.
8. Sakao, S., Tatsumi, K., and Voelkel, N.F. (2009). Endothelial cells and pulmonary arterial hypertension: apoptosis, proliferation, interaction and transdifferentiation. Respir. Res. *10*, 95.
9. Fatica, A., and Bozzoni, I. (2014). Long non-coding RNAs: new players in cell differentiation and development. Nat. Rev. Genet. *15*, 7–21.
10. St Laurent, G., Wahlestedt, C., and Kapranov, P. (2015). The Landscape of long noncoding RNA classification. Trends Genet. *31*, 239–251.
11. Mercer, T.R., Dinger, M.E., and Mattick, J.S. (2009). Long non-coding RNAs: insights into functions. Nat. Rev. Genet. *10*, 155–159.
12. Ponting, C.P., Oliver, P.L., and Reik, W. (2009). Evolution and functions of long noncoding RNAs. Cell *136*, 629–641.
13. Ji, P., Diederichs, S., Wang, W., Böing, S., Metzger, R., Schneider, P.M., Tidow, N., Brandt, B., Buerger, H., Bulk, E., et al. (2003). MALAT-1, a novel noncoding RNA, and thymosin beta4 predict metastasis and survival in early-stage non-small cell lung cancer. Oncogene *22*, 8031–8041.
14. Mercer, T.R., and Mattick, J.S. (2013). Structure and function of long noncoding RNAs in epigenetic regulation. Nat. Struct. Mol. Biol. *20*, 300–307.
15. Yoon, J.H., Abdelmohsen, K., and Gorospe, M. (2013). Posttranscriptional gene regulation by long noncoding RNA. J. Mol. Biol. *425*, 3723–3730.
16. Wiles, M.V. (1988). Isolation of differentially expressed human cDNA clones: similarities between mouse and human embryonal carcinoma cell differentiation. Development *104*, 403–413.
17. Pachnis, V., Brannan, C.I., and Tilghman, S.M. (1988). The structure and expression of a novel gene activated in early mouse embryogenesis. EMBO J. *7*, 673–681.
18. Gabory, A., Ripoche, M.A., Le Digarcher, A., Watrin, F., Ziyyat, A., Forné, T., Jammes, H., Ainscough, J.F., Surani, M.A., Journot, L., and Dandolo, L. (2009). H19 acts as a trans regulator of the imprinted gene network controlling growth in mice. Development *136*, 3413–3421.
19. Hourihan, R.N., O'Sullivan, G.C., and Morgan, J.G. (2003). Transcriptional gene expression profiles of oesophageal adenocarcinoma and normal oesophageal tissues. Anticancer Res. *23* (1A), 161–165.
20. Torres, F., González-Candia, A., Montt, C., Ebensperger, G., Chubretovic, M., Serón-Ferré, M., Reyes, R.V., Llanos, A.J., and Herrera, E.A. (2015). Melatonin reduces oxidative stress and improves vascular function in pulmonary hypertensive newborn sheep. J. Pineal Res. *58*, 362–373.
21. Jin, H., Wang, Y., Zhou, L., Liu, L., Zhang, P., Deng, W., and Yuan, Y. (2014). Melatonin attenuates hypoxic pulmonary hypertension by inhibiting the inflammation and the proliferation of pulmonary arterial smooth muscle cells. J. Pineal Res. *57*, 442–450.
22. Stenmark, K.R., Fagan, K.A., and Frid, M.G. (2006). Hypoxia-induced pulmonary vascular remodeling: cellular and molecular mechanisms. Circ. Res. *99*, 675–691.
23. Costa, E.J., Lopes, R.H., and Lamy-Freund, M.T. (1995). Permeability of pure lipid bilayers to melatonin. J. Pineal Res. *19*, 123–126.
24. Cai, B., Ma, W., Bi, C., Yang, F., Zhang, L., Han, Z., Huang, Q., Ding, F., Li, Y., Yan, G., et al. (2016). Long noncoding RNA H19 mediates melatonin inhibition of premature senescence of c-kit(+) cardiac progenitor cells by promoting miR-675. J. Pineal Res. *61*, 82–95.
25. Liang, W.C., Fu, W.M., Wong, C.W., Wang, Y., Wang, W.M., Hu, G.X., Zhang, L., Xiao, L.J., Wan, D.C., Zhang, J.F., and Waye, M.M. (2015). The lncRNA H19 promotes epithelial to mesenchymal transition by functioning as miRNA sponges in colorectal cancer. Oncotarget *6*, 22513–22525.
26. Rabinovitch, M., Gamble, W., Nadas, A.S., Miettinen, O.S., and Reid, L. (1979). Rat pulmonary circulation after chronic hypoxia: hemodynamic and structural features. Am. J. Physiol. *236*, H818–H827.
27. Hung, M.W., Yeung, H.M., Lau, C.F., Poon, A.M.S., Tipoe, G.L., and Fung, M.L. (2017). Melatonin Attenuates Pulmonary Hypertension in Chronically Hypoxic Rats. Int. J. Mol. Sci. *18*, E1125.
28. Cai, X., and Cullen, B.R. (2007). The imprinted H19 noncoding RNA is a primary microRNA precursor. RNA *13*, 313–316.
29. Tsang, W.P., Ng, E.K., Ng, S.S., Jin, H., Yu, J., Sung, J.J., and Kwok, T.T. (2010). Oncofetal H19-derived miR-675 regulates tumor suppressor RB in human colorectal cancer. Carcinogenesis *31*, 350–358.
30. Keniry, A., Oxley, D., Monnier, P., Kyba, M., Dandolo, L., Smits, G., and Reik, W. (2012). The H19 lincRNA is a developmental reservoir of miR-675 that suppresses growth and Igf1r. Nat. Cell Biol. *14*, 659–665.
31. Arnqvist, H.J. (2008). The role of IGF-system in vascular insulin resistance. Horm. Metab. Res. *40*, 588–592.
32. Badesch, D.B., Lee, P.D., Parks, W.C., and Stenmark, K.R. (1989). Insulin-like growth factor I stimulates elastin synthesis by bovine pulmonary arterial smooth muscle cells. Biochem. Biophys. Res. Commun. *160*, 382–387.
33. Joss-Moore, L.A., Albertine, K.H., and Lane, R.H. (2011). Epigenetics and the developmental origins of lung disease. Mol. Genet. Metab. *104*, 61–66.
34. Perkett, E.A., Badesch, D.B., Roessler, M.K., Stenmark, K.R., and Meyrick, B. (1992). Insulin-like growth factor I and pulmonary hypertension induced by continuous air embolization in sheep. Am. J. Respir. Cell Mol. Biol. *6*, 82–87.

35. Lankat-Buttgereit, B., and Göke, R. (2003). Programmed cell death protein 4 (pdcd4): a novel target for antineoplastic therapy? Biol. Cell *95*, 515–519.

36. Lankat-Buttgereit, B., and Göke, R. (2009). The tumour suppressor Pdcd4: recent advances in the elucidation of function and regulation. Biol. Cell *101*, 309–317.

37. Liu, X., Cheng, Y., Yang, J., Krall, T.J., Huo, Y., and Zhang, C. (2010). An essential role of PDCD4 in vascular smooth muscle cell apoptosis and proliferation: implications for vascular disease. Am. J. Physiol. Cell Physiol. *298*, C1481–C1488.

38. Young, M.R., Yang, H.S., and Colburn, N.H. (2003). Promising molecular targets for cancer prevention: AP-1, NF-kappa B and Pdcd4. Trends Mol. Med. *9*, 36–41.

39. Kurihara, H., Yoshizumi, M., Sugiyama, T., Yamaoki, K., Nagai, R., Takaku, F., Satoh, H., Inui, J., Yanagisawa, M., Masaki, T., and Yazaki, Y. (1989). The possible role of endothelin-1 in the pathogenesis of coronary vasospasm. J. Cardiovasc. Pharmacol. *13*, S132–S137.

40. Sakao, S., Taraseviciene-Stewart, L., Lee, J.D., Wood, K., Cool, C.D., and Voelkel, N.F. (2005). Initial apoptosis is followed by increased proliferation of apoptosis-resistant endothelial cells. FASEB J. *19*, 1178–1180.

41. Davis, B.N., Hilyard, A.C., Lagna, G., and Hata, A. (2008). SMAD proteins control DROSHA-mediated microRNA maturation. Nature *454*, 56–61.

42. Mudduluru, G., George-William, J.N., Muppala, S., Asangani, I.A., Kumarswamy, R., Nelson, L.D., and Allgayer, H. (2011). Curcumin regulates miR-21 expression and inhibits invasion and metastasis in colorectal cancer. Biosci. Rep. *31*, 185–197.

43. Green, D.E., Murphy, T.C., Kang, B.Y., Searles, C.D., and Hart, C.M. (2015). PPARγ Ligands Attenuate Hypoxia-Induced Proliferation in Human Pulmonary Artery Smooth Muscle Cells through Modulation of MicroRNA-21. PLoS ONE *10*, e0133391.

44. Ji, R., Cheng, Y., Yue, J., Yang, J., Liu, X., Chen, H., Dean, D.B., and Zhang, C. (2007). MicroRNA expression signature and antisense-mediated depletion reveal an essential role of MicroRNA in vascular neointimal lesion formation. Circ. Res. *100*, 1579–1588.

45. Li, X., Huang, K., and Yu, J. (2014). Inhibition of microRNA-21 upregulates the expression of programmed cell death 4 and phosphatase tensin homologue in the A431 squamous cell carcinoma cell line. Oncol. Lett. *8*, 203–207.

46. Sarkar, J., Gou, D., Turaka, P., Viktorova, E., Ramchandran, R., and Raj, J.U. (2010). MicroRNA-21 plays a role in hypoxia-mediated pulmonary artery smooth muscle cell proliferation and migration. Am. J. Physiol. Lung Cell. Mol. Physiol. *299*, L861–L871.

47. White, K., Dempsie, Y., Caruso, P., Wallace, E., McDonald, R.A., Stevens, H., Hatley, M.E., Van Rooij, E., Morrell, N.W., MacLean, M.R., and Baker, A.H. (2014). Endothelial apoptosis in pulmonary hypertension is controlled by a microRNA/programmed cell death 4/caspase-3 axis. Hypertension *64*, 185–194.

48. Riley, D.J., Thakker-Varia, S., Wilson, F.J., Poiani, G.J., and Tozzi, C.A. (2000). Role of proteolysis and apoptosis in regression of pulmonary vascular remodeling. Physiol. Res. *49*, 577–585.

49. Morrell, N.W., Adnot, S., Archer, S.L., Dupuis, J., Jones, P.L., MacLean, M.R., McMurtry, I.F., Stenmark, K.R., Thistlethwaite, P.A., Weissmann, N., et al. (2009). Cellular and molecular basis of pulmonary arterial hypertension. J. Am. Coll. Cardiol. *54* (1, Suppl), S20–S31.

50. Meyrick, B., and Reid, L. (1980). Hypoxia-induced structural changes in the media and adventitia of the rat hilar pulmonary artery and their regression. Am. J. Pathol. *100*, 151–178.

51. Barman, S.A., Chen, F., Su, Y., Dimitropoulou, C., Wang, Y., Catravas, J.D., Han, W., Orfi, L., Szantai-Kis, C., Keri, G., et al. (2014). NADPH oxidase 4 is expressed in pulmonary artery adventitia and contributes to hypertensive vascular remodeling. Arterioscler. Thromb. Vasc. Biol. *34*, 1704–1715.

52. Cowan, K.N., Heilbut, A., Humpl, T., Lam, C., Ito, S., and Rabinovitch, M. (2000). Complete reversal of fatal pulmonary hypertension in rats by a serine elastase inhibitor. Nat. Med. *6*, 698–702.

53. Nishimura, T., Vaszar, L.T., Faul, J.L., Zhao, G., Berry, G.J., Shi, L., Qiu, D., Benson, G., Pearl, R.G., and Kao, P.N. (2003). Simvastatin rescues rats from fatal pulmonary hypertension by inducing apoptosis of neointimal smooth muscle cells. Circulation *108*, 1640–1645.

54. McMurtry, M.S., Bonnet, S., Wu, X., Dyck, J.R., Haromy, A., Hashimoto, K., and Michelakis, E.D. (2004). Dichloroacetate prevents and reverses pulmonary hypertension by inducing pulmonary artery smooth muscle cell apoptosis. Circ. Res. *95*, 830–840.

55. Wang, R., Zhou, S.J., Zeng, D.S., Xu, R., Fei, L.M., Zhu, Q.Q., Zhang, Y., and Sun, G.Y. (2014). Plasmid-based short hairpin RNA against connective tissue growth factor attenuated monocrotaline-induced pulmonary vascular remodeling in rats. Gene Ther. *21*, 931–937.

56. Zhou, S., Sun, L., Cao, C., Wu, P., Li, M., Sun, G., Fei, G., Ding, X., and Wang, R. (2018). Hypoxia-induced microRNA-26b inhibition contributes to hypoxic pulmonary hypertension via CTGF. J. Cell. Biochem. *119*, 1942–1952.

57. Ding, X., Zhou, S., Li, M., Cao, C., Wu, P., Sun, L., Fei, G., and Wang, R. (2017). Upregulation of SRF Is Associated With Hypoxic Pulmonary Hypertension by Promoting Viability of Smooth Muscle Cells via Increasing Expression of Bcl-2. J. Cell. Biochem. *118*, 2731–2738.

58. Wang, R., Ding, X., Zhou, S., Li, M., Sun, L., Xu, X., and Fei, G. (2016). Microrna-26b attenuates monocrotaline-induced pulmonary vascular remodeling via targeting connective tissue growth factor (CTGF) and cyclin D1 (CCND1). Oncotarget *7*, 72746–72757.

59. Wang, R., Xu, Y.J., Liu, X.S., Zeng, D.X., and Xiang, M. (2012). CCN2 promotes cigarette smoke-induced proliferation of rat pulmonary artery smooth muscle cells through upregulating cyclin D1 expression. J. Cell. Biochem. *113*, 349–359.

60. Zhou, S.J., Li, M., Zeng, D.X., Zhu, Z.M., Hu, X.W., Li, Y.H., Wang, R., and Sun, G.Y. (2015). Expression variations of connective tissue growth factor in pulmonary arteries from smokers with and without chronic obstructive pulmonary disease. Sci. Rep. *5*, 8564.

61. Zhou, S., Li, M., Zeng, D., Xu, X., Fei, L., Zhu, Q., Zhang, Y., and Wang, R. (2015). A single nucleotide polymorphism in 3′ untranslated region of epithelial growth factor receptor confers risk for pulmonary hypertension in chronic obstructive pulmonary disease. Cell. Physiol. Biochem. *36*, 166–178.

62. Wang, R., Li, M., Zhou, S., Zeng, D., Xu, X., Xu, R., and Sun, G. (2015). Effect of a single nucleotide polymorphism in miR-146a on COX-2 protein expression and lung function in smokers with chronic obstructive pulmonary disease. Int. J. Chron. Obstruct. Pulmon. Dis. *10*, 463–473.

63. Zhou, S., Li, M., Zeng, D., Sun, G., Zhou, J., and Wang, R. (2015). Effects of basic fibroblast growth factor and cyclin D1 on cigarette smoke-induced pulmonary vascular remodeling in rats. Exp. Ther. Med. *9*, 33–38.

64. Wang, R., Xu, Y.J., Liu, X.S., Zeng, D.X., and Xiang, M. (2011). Knockdown of connective tissue growth factor by plasmid-based short hairpin RNA prevented pulmonary vascular remodeling in cigarette smoke-exposed rats. Arch. Biochem. Biophys. *508*, 93–100.

65. Zhou, S., Liu, Y., Li, M., Wu, P., Sun, G., Fei, G., Xu, X., Zhou, X., Zhou, L., and Wang, R. (2018). Combined Effects of PVT1 and MiR-146a Single Nucleotide Polymorphism on the Lung Function of Smokers with Chronic Obstructive Pulmonary Disease. Int. J. Biol. Sci. *14*, 1153–1162.